Published in Journal of Cleaner Production with doi: 10.1016/j.jclepro.2022.133558

A Three-Stage Stochastic-IGDT Model for Photovoltaic-Battery Domestic Systems Considering Outages and Real-Time Pricing

Marcos-Tostado Véliz[1], Bablesh Kumar Jha[2], Salah Kamel[3], Naran M. Pindoriya[2], Francisco Jurado[1,*]

1. Department of Electrical Engineering, University of Jaén, 23700 Linares, Spain (e-mail: mtostado@ujaen.es (M.T.-V.), fjurado@ujaen.es (F.J.)).
2. Department of Electrical Engineering, Indian Institute of Technology Gandhinagar (e-mail: bablesh.j@iitgn.ac.in (B.K.J.), naran@iitgn.ac.in (N.M.P.))
3. Department of Electrical Engineering, Faculty of Energy Engineering, Aswan University, Aswan 81528, Egypt (e-mail: skamel@aswu.edu.eg)

* Correspondence: fjurado@ujaen.es

Abstract - Energy consumption from residential sector is a growing concern nowadays. It has been widely demonstrated that domestic consumption worldwide could be notably reduced implementing home energy management tools. This kind of programs allows to schedule the different controllable home assets to optimize the electricity bill and increment the penetration of onsite renewable technologies, which contributes to a further reduction in residential consumption. On the other hand, grid outages are still frequent nowadays because natural disasters or weak infrastructures. Therefore, home energy management tools do not ignore these events. To tackle this issue, this paper develops a novel three-stage solution procedure for home energy management problems considering grid outages. To this end, a novel stochastic-IGDT formulation of the home energy management problem is proposed, by which the uncertain parameters are incorporated via scenarios and grid outages are modelled using IGDT. The presented formulation is Mixed-Integer Linear programming and allows to obtain a schedule result for the home appliances immune against outages without ignoring the economy of the system. A benchmark prosumer environment with Real-Time pricing is considered as a case study. The results prove the effectiveness of the developed methodology. In particular, the effectiveness of the developed formulation in modelling grid outages as well as the scheduling performance at different conflictive objectives are highlighted. In addition, the effect of primarily considering robustness or economy is discussed together the importance of onsite photovoltaic generation in incrementing the reliability of the home system. Finally, the capability of the developed procedure to jointly consider cost and outages on a whole is foregrounded. In fact, the developed methodology is able to assume up to 6.5 outage hours without increasing the electricity bill, thus evidencing its capability to obtain a result immune against outages, whereas economic concerns are also considered on a whole.

Keywords - renewable energy; home energy management; grid outage; real-time pricing; battery energy storage.

Nomenclature

Indices (Sets)

Ω	Cluster of a representative scenario
$k(\mathcal{K}^{\mathrm{NI}}/\mathcal{K}^{\mathrm{I}})$	Non-interruptible/interruptible controllable appliances
$r(\mathcal{R})$	Representative scenario
$s(\mathcal{S})$	Scenario
$t(\mathcal{T})$	Time
Ψ	Time window of a controllable appliance

Superscripts

$BES, ch/dch$	Battery energy storage in charging/discharging mode
$Grid, b/s$	Bought/sold from/to the utility grid
EWH	Electric water heater
$HVAC, h/c$	Heating-ventilation-air conditioner system in heating/cooling mode
$w, h/c$	Hot/cold water
$\underline{(*)}/\overline{(*)}$	Minimum/maximum value of a variable/parameter
NC	Non-controllable appliances
$Air, out/in$	Outside/inside air
PV	Photovoltaic array
PEV	Plug-in electric vehicle
sp/db	Set-point/dead-band
$\widehat{(*)}$	Uncertain parameter

Constants and parameters

C	Coefficient of performance (pu)
δ	Duty cycle of a controllable appliance (-)
η	Efficiency (pu)
λ	Energy price ($/kWh)
R	Equivalent thermal resistance of the building (kW/ºC)
Q	Heat or thermal capacity ($\mathrm{kJ}/(\mathrm{kg}\cdot{}^{\circ}\mathrm{C})$ or kWh/ºC)
μ	Life-cycle cost of BES ($\$/\mathrm{kWh}^2$)
m	Mass (kg)
π	Probability (pu)
ϑ	Solar irradiation ($\mathrm{kW/m}^2$)
θ	Temperature (ºC)
$\Delta\tau$	Time step (h)
v	Water volume (gal)

Decision variables ($\boldsymbol{x}$)

on/off	Activation/deactivation status (binary)
u	Commitment status (binary)
ε	Energy stored (kWh)
p	Power (kW)

1 – Introduction

1.1 - Background & Motivation

Residential buildings account for nearly two-thirds of total primary energy use in Europe [1]. In Europe, building energy consumption is 40–42 %, with 35–40 % related to CO2 emissions [2, 3]. However, the energy savings potential in [2] is projected to be between 27 and 30 %. Due to worries about global warming and energy scarcity, a home energy management (HEM) system is becoming more significant. This system helps reduce electricity usage, particularly during peak load hours, and increment the use of onsite renewable generators such as photovoltaic (PV) arrays.

HEM tools should be considered not just as a technique to cut greenhouse gas emissions, but also as a way to automate power management in a home. These programs can be implemented in residential houses to assist in power management by interacting with household appliances and utilities, monitoring energy usage, and receiving information (such as tariff pricing) to reduce power consumption by scheduling the use of household equipment [4]. In practise, however, the variety of home users' electrical equipment, the complexity of the operational status of numerous devices, and the uncertainty of home users' electricity consumption habits have all posed significant hurdles to HEM dispatching. Thus, HEM systems in particular have gotten a lot of interest in academia and industry in recent years.

According to [5], a power outage has a tremendous economic impact, with eight important U.S. market segments losing nearly $27 billion per year due to outages. To minimise the impact of disruptions, more than ever, require energy management systems to balance and even out demand spikes or supply dips. In this sense, HEM tools would help to optimize the use of rooftop PV installations in order to increment the reliability of the system and its immunity against outages, thus reducing their impact on inhabitants’ economy and welfare. To maximise energy savings and assure customer satisfaction, the HEM system employs optimal scheduling and advanced control mechanisms. To tackle the home optimal scheduling problem, it is critical to handle efficient and practical way for power outage also.

1.2 - Related works

The literature on HEM problem, design and development is substantial, with some representative publications mentioned below. Different HEM models can be created to manage various types of residential assets. Some HEM systems are designed to schedule thermostatically controlled appliances in the most efficient way possible. Various programmable household appliances, renewable energy sources, and energy storage technologies are all coordinated in some research activities [6-8]. Authors of [9], suggested a scheduling model to schedule household appliance operations best under day-ahead anticipated real-time pricings (RTPs). Under an RTP scheme, reference [10] presented a HEM tool that optimally schedules the operation of household appliances. Authors of [11] present a HEM model for energy optimization and group household appliances into categories. The suggested model's main goal is to lower power costs by addressing the uncertainties associated with various types of loads. The proposed algorithms are put to the test by examining the required household equipment as well as the day-ahead pricing structure. In [12], a HEM model was developed that kept consumers comfortable by attempting to lower the total bill while meeting the consumer's electricity bill target, thus relaxing the optimization problem. The mathematical modelling of HEM with small-scale renewable energy sources was explored in [13]. The proposed model aims to intelligently control household load demand in order to concurrently minimise both the customer's energy bill and the network's peak demand. The authors in [14] transformed the HEM optimization problem from a single-time scale to a multi-time scale in order to save computational time. In [15], the authors developed a multi-objective model for HEM systems, with two primary objectives: the consumer's energy bill and peak load demand, and the problem was reduced to a single-objective problem using the weighted sum technique. In [16], a HEM architecture that comprises optimal DR and increased PV self-consumption has been presented to reduce the total daily household energy bills. The proposed approach presents scheduling of various types of flexible electrical loads (i.e. TSAs, TCAs, and PSAs) and responding to B2X and V2X technologies. They have also considered the battery degradation cost to the optimization framework. To offer flexibility in demand side energy management, they used smart thermostats with an adjustable set-point rather than the fixed set-point thermostats. In multi-carrier energy hubs, a distributed transactive energy model based on mixed-integer linear program (MILP) that reduces total load demand and consequently overall cost and power losses, has been proposed in [17]. Both analyses, however, failed to account for the possibility of outage survival. Through a centralised coordinated HEM, a market-based solution to mitigate distribution network congestions has been proposed in [18]. They used Dynamic Tariffs (DT) and Daily Power-based Network Tariffs (DPT) to manage congestion caused by electric vehicles (EVs) and heat pumps (HPs) in the distribution system without compromising the comfort and convenience of the energy consumers. In [19], a multi-carrier energy microgrid (mMG) has been proposed in which authors have integrated the electricity and gas networks during numerous significant grid outages. The bi-level optimization strategy has been proposed to enhance the system resiliency by ensuring energy and heat demand during an emergency while minimizing operational expenses. In [20], a robust sizing technique and energy management system for a mMG has been developed to harness the resilience benefits, considering photovoltaics, conventional power sources with energy storage units. The proposed approach has been validated on the test-rig developed at Californian hospital. Their results show the grid resiliency in sustaining a continuous energy supply in the case of grid outage at various periods throughout the year while minimizing the operational cost. From [21], the capacity of PV generation and plug-in electric vehicles (PEV) can affect a smart home's backup capability during an electric outage. For the sake of simplicity, the taxonomy of relevant literature is given in Table 1.

Table 1. Taxonomy of relevant literature

Ref.	Optimization Modelling	Uncertainty	Grid outage	Remarks
[6]	Bio-inspired	No	No	A multi-objective optimization method that considers two main purposes including energy consumption cost and user satisfaction
[7]	Mixed-integer linear programming (MILP)	No	No	MILP-based HEM system performs day-ahead load scheduling for cost-minimization
[9]	Bio-inspired	No	No	Combined RTP with the inclining block rate model are adopted for reducing electricity expense and alleviating the power peak-to-average ratio
[13]	MILP, Game theory	Yes (For load)	No	Minimise both the consumer's energy bill and the system peak demand simultaneously
[14]	Cooperative particle swarm optimization	No	No	Problem’s transformation from single-time scale to multi-time scale to minimize total electricity cost and user discomfort of temperature
[16]	MILP, metaheuristic algorithm	Yes	Yes	Stochastic programming approach based on Wasserstein distance metric and K-medoids based is applied to handle the residential photovoltaic solar power uncertainty
[17]	NAA Solver, Mosel optimisation toolbox	Yes	Yes	Proposes a hierarchical energy management scheme for residential communities, aiming to facilitate energy sharing among houses and minimize the impact on the grid outage on the whole community
This Paper	MILP, Stochastic, Information gap decision theory (IGDT)	Yes	Yes	A novel stochastic-IGDT formulation of the home energy management problem is proposed, by which the uncertain parameters are incorporated via scenarios and grid outages are modelled using IGDT.

The majority of the aforementioned research papers [9-21] focus on HEM models that are scheduled a day ahead of time. Only a few studies exist that address the grid outages issue with HEM system [22-25]. In [22], a home resilient energy management system (HREMS) has been proposed to reduce grid power dependency during grid outage by optimal scheduling of energy assets. In this study, the Wasserstein distance metric and a K-medoids-based scenario analysis technique have been used to consider the uncertainties related to renewable generation. The calculation of energy cost has not been considered in this work which lacks the complete techno-economic analysis of the adopted HREMS. Reducing dependence on grid power during blackouts is one of the reliability criteria for a household that helps to make a viable economic decision regarding the economic burden. Thus, the energy cost calculation is necessary beforehand to implement such HREMS. In [23], an energy management system is proposed to achieve a social warfare goal by reducing the community's unreserved load over the intended planned outage. The proposed tool decomposes the energy management workflow into two levels to address the complexity produced by a large number of domestic energy resources present in many dwellings. During power outages, an energy management solution for residential consumers with energy assets such as electric vehicles and smart home equipment is recommended in [24]. Its goal is to increase the energy resilience of such households by allowing the vehicle to deliver power via vehicle-to-home technology. This technique allows for a minimum level of comfort to be maintained during the outage, as well as the control of selected loads and appliances. However, in [23]- [24], the renewable energy sources, such as solar PV, and the associated uncertainties have not been considered in the mathematical framework. Hence, the uncertainties related to renewable energy would have a substantial impact on residential energy management decisions, which would be especially apparent in the event of a power outage. Indeed, the lack of renewable integration lacks the true picture of a realistic scenario. To tackle power outages, authors of [25] has proposed an energy management solution such as peer-to-peer operation, electrical car charging-discharging, partial charge capability, load reduction, and load modification are the alternatives. The goal is to reduce energy costs while also increasing energy resilience in the event of a various power outage. They have considered the load curtailment scheme without consideration of RTP, which reduces the home energy consumption up-to 90% which shows that the adopted approach did not consider the consumers' comfort levels. Hence, the energy management solution without consideration of real-time pricing model and consumer comfort level seems to be hypothetical work.

1.3 - Research Gaps

On the basis of the literature above, it can be extracted various research gaps, which has motivated the present work:

- In most of the literature, grid is considered available anytime. In other words, grid failures are not considered in HEM problems. This assumption may lead to unrealistic scheduling results, that can harm the monetary expenditures of home inhabitants at last. In this regard, it is necessary to consider possible blackouts in order to reproduce a HEM scheduling plan immune against outages.
- Most of the related literature focuses on simple uncertainties modelling, adopting only one model for all the uncertainties involved in most of cases. This assumption may be invalid when the uncertainties have different features. For example, in case of grid outages, it cannot be easily predicted with accuracy.

1.4 - Contribution

This paper aims at overcoming some of the limitations of existing literature. As seen in Table 1, this reference is the most completed one and, for the first time, a novel stochastic-IGDT approach is applied to HEM problems in order to consider both uncertainties and grid outages. The main contributions of the present paper are summarized below, for simplicity.

- Developing a novel HEM model considering grid outages. In contrast to other approaches, the developed model is a MILP. This kind of formulation is normally preferred since these problems can be solved with standard solvers, is versatile and modular, can be efficiently attached and ensure the reachability of the global optimum [26].
- Proposing a novel formulation based on stochastic-IGDT modelling, which jointly considers uncertainties from renewable generation, weather parameters, time-varying house demand and RTP, as well as grid outages. In contrast to other approaches, in the developed model the electricity bill is also considered, so that immunity against outages is not achieved at expenses of inadmissibly incrementing the energy cost. In addition, the consideration of weather uncertainties together other unpredictable patterns provides a better management of onsite renewable generators, thus using them to improve both economy and reliability of the system on a whole.
- Developing a novel three-stage solution procedure based on the proposed model for HEM problems. The developed multi-stage algorithm aims at properly managing grid outages as an uncertain using IGDT. This way, the different stages are devoted on calculating the bounds of the concerned uncertainty, as explained throughout this paper.

To prove the effectiveness of the developed tool, extensive simulations are performed on a benchmark prosumer environment, providing and discussing several numerical results.

1.5 - Organisation of paper

The rest of this paper is organized in the following manner. The description of the considered home system is presented in the next section. Mathematical framework for HEM system is discussed in Section 3. Section 4 describes the adopted solution techniques considering uncertainty related to HEM tools. Afterward, to validate the proposed approach, case studies are introduced in Section 5. Finally, Section 6 concludes this paper.

2 - Description of the considered home system

This paper focuses on a benchmark prosumer layout as pictorially represented in Fig. 1. The system can be supplied from the utility grid or by means of onsite assets. In this sense, a battery energy storage (BES) unit is deployed along a photovoltaic (PV) array for self-supplying the installation. The battery bank allows a more efficient management of renewable generation [27, 28], but also of the energy purchased from the grid, which has a cost per kWh determined by RTP tariff. Thereby, energy can be purchased during low-price hours and stored to partially or entirely cover the home demand during peak-price periods. The system also allows to sell back energy to the utility grid and thus to get a monetary revenue [29].

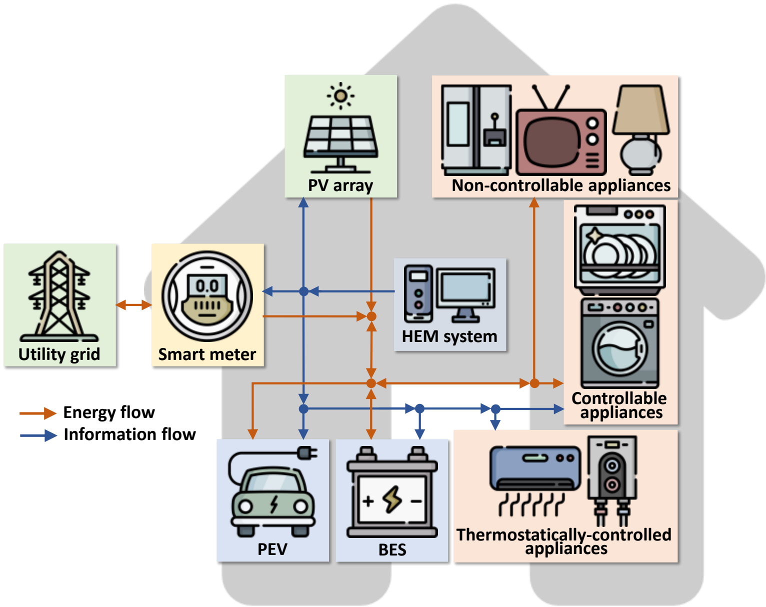

Fig. 1 - Pictorial representation of the home system under study

The home demand is composed by a set of domestic appliances, which can be categorized into different groups. The non-controllable appliances are operated under human decisions and therefore they cannot be scheduled. In contrast, the controllable appliances can be scheduled within predefined time windows on pursuing a more efficient home energy management. As customary, the controllable appliances are divided into interruptible, non-interruptible and thermostatically-controlled (see [30] for further details). Finally, it is assumed that the house incorporates a unidirectional charger for plug-in electric vehicles (PEVs). This installation is devoted on charging the on-board BES during the hours in which the vehicle is parked at home.

The scheduling of the different controllable assets is determined by a HEM system. As commented, this kind of program is able to determine the day-ahead scheduling plan of the different domestic devices according a specific objective function (typically the energy cost [31]). The scheduling process of the HEM is illustrated in Fig. 2. Let us assume that forecast information of different uncertain parameters (such as weather or RTP) is available with sufficient accuracy sometime the day before of the scheduling realization. This is a plausible assumption given the vast availability of advanced forecast techniques [32, 33], that are capable to predict the concerned unknowns with day-ahead precision easily. This information along some other preferences (e.g. temperature set-points) serve then as inputs of the HEM tool. Making use of this information, the HEM system determines the optimal scheduling plan for the controllable appliances, energy exchanging with the utility grid and onsite generation/storage assets. As one of the main contributions of this paper, the developed HEM system will be able to produce a scheduling profile immune against outages, as explained in Section 4.

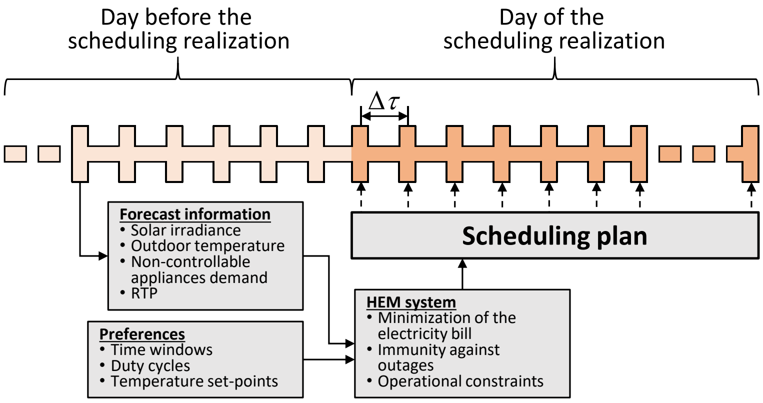

Fig. 2 - Sketch of the HEM scheduling process

3 - Mathematical models

In this section, the mathematical models of the different home components are presented. These models are incorporated into the HEM optimization problem as constraints (see Section 4). All the formulation here presented is MILP, thus ensuring the global-optimal reachability using standard solvers [34].

3.1 - Utility grid modelling

The utility grid can be modelled by the constraints (1) and (2), which limit the power that can be purchased/sold from/to the grid and make the buying and selling processes complementary, respectively.

$$p_{r|t}^{Grid,i} \leq u_t^{Grid,i} \cdot \overline{p}^{Grid}; \; \forall r \in \mathcal{R} \wedge t \in \mathcal{T} \wedge i \in \{b,s\} \quad (1)$$

$$u_t^{Grid,b} + u_t^{Grid,s} \leq 1; \; \forall r \in \mathcal{R} \wedge t \in \mathcal{T} \quad (2)$$

It is noteworthy that the model above considers total availability of the grid (no grid outages). This phenomenon is modelled in Section 4.

3.2 - PV array modelling

Potential PV generation depends on weather conditions, especially solar irradiance and ambient temperature [35]. These two factors can be converted to PV power using the expression (3) [36].

$$\phi_{r|t}^{PV} = \overline{p}^{PV} \cdot \left[0.25 \cdot \hat{\vartheta}_{r|t} + 0.03 \cdot \hat{\vartheta}_{r|t} \cdot \hat{\theta}_{r|t}^{Air,out} + (1.01 - 1.13 \cdot \eta^{PV}) \cdot \hat{\vartheta}_{r|t}^{2}\right];\ \forall r \in \mathcal{R} \wedge t \in \mathcal{T} \tag{3}$$

In this paper, both solar irradiance and ambient temperature are considered unknown and therefore they are modelled as uncertain parameters in (3). As mentioned in some references (e.g. see [35]), the model (3) should be complemented with the constraint (4), since it may yield a PV potential superior than the array nominal power.

$$p_{r|t}^{PV} \leq \begin{cases} \phi_{r|t}^{PV}, & \text{if } \phi_{r|t}^{PV} \leq 1.1 \cdot \overline{p}^{PV} \\ 1.1 \cdot \overline{p}^{PV}, & \text{otherwise} \end{cases};\ \forall r \in \mathcal{R} \wedge t \in \mathcal{T} \tag{4}$$

Indeed, the expression (4) limits the PV generation by 10% over the nominal value, which can be considered acceptable in practise [35].

3.3 - BES modelling

The expression (5) upper bounds the power that the BES can exchange with the home to nominal values (normally determined by its nominal capacity and the so-called energy-to-power ratio [37]). On the other hand, the constraint (6) avoids the simultaneous charging and discharging of the batteries.

$$p_{r|t}^{BES,i} \leq u_{t}^{BES,i} \cdot \bar{p}^{BES};\ \forall r \in \mathcal{R} \wedge t \in \mathcal{T} \wedge i \in \{ch, dch\} \tag{5}$$

$$u_{t}^{BES,ch} + u_{t}^{BES,dch} \leq 1;\ \forall t \in \mathcal{T} \tag{6}$$

The energy stored in the BES is modelled by (7). This expression determines the state-of-charge (SOC) at any time instant as a function of the SOC at the previous time slot and the energy exchanged with the home [37]. To be realistic, the constraint (8) bounds the energy stored in batteries to nominal values and depth-of-discharge settings.

$$\varepsilon_{r|t}^{BES} = \varepsilon_{r|t-1}^{BES} + \Delta\tau \cdot \left(\eta^{BES} \cdot p_{r|t}^{BES,ch} - {p_{r|t}^{BES,dch}}\Big/{\eta^{BES}}\right);\ \forall r \in \mathcal{R} \wedge t \in \mathcal{T} \backslash t > 1 \tag{7}$$

$$\underline{\varepsilon}^{BES} \leq \varepsilon_{r|t}^{BES} \leq \bar{\varepsilon}^{BES};\ \forall r \in \mathcal{R} \wedge t \in \mathcal{T} \tag{8}$$

Since the model (7) is not defined at $t = 1$, the expression (9) is declared to set the initial SOC. To keep the model coherent, the final SOC is fixed equal to the nominal capacity.

$$\varepsilon_{r|\mathcal{T}(1)}^{BES} = \varepsilon_{r|\mathcal{T}(\text{end})}^{BES} = \bar{\varepsilon}^{BES};\ \forall r \in \mathcal{R} \tag{9}$$

3.4 - PEV modelling

In contrast to the stationary BES, which is available at any time, the PEV cannot be charged at any moment because either it is not parked at home or some energy management system avoids its charging during non-suitable hours [38]. The expressions (10) and (11) model this limitation considering the time window Ψ^{PEV}, which corresponds to the time slots in which the PEV charging is enabled.

$$p_{r|t}^{PEV} \leq \bar{p}^{PEV};\ \forall r \in \mathcal{R} \wedge t \in \Psi^{PEV} \tag{10}$$

$$p_{r|t}^{PEV} = 0;\ \forall r \in \mathcal{R} \wedge t \notin \Psi^{PEV} \tag{11}$$

Indeed, the model above forces the PEV demand to be zero when the charging process is disabled. On the other hand, equations (12) and (13) are analogue to (7) and (8) but referred to the on-board battery pack. Finally, equation (14) forces to fully charge the PEV within the preestablished time window.

$$\varepsilon_{r|t}^{PEV} = \varepsilon_{r|t-1}^{PEV} + \Delta\tau \cdot \eta^{PEV} \cdot p_{r|t}^{PEV};\ \forall r \in \mathcal{R} \wedge t \in \mathcal{T} \backslash t > 1 \tag{12}$$

$$\underline{\varepsilon}^{PEV} \leq \varepsilon_{r|t}^{PEV} \leq \bar{\varepsilon}^{PEV};\ \forall r \in \mathcal{R} \wedge t \in \mathcal{T} \tag{13}$$

$$\varepsilon_{r|\Psi^{PEV}(\text{end})}^{PEV} = \bar{\varepsilon}^{PEV};\ \forall r \in \mathcal{R} \tag{14}$$

3.5 - Controllable appliances modelling

The controllable appliances must complete their duty cycles within the established time windows, being not possible to schedule them within other time slots, as said the constraints (15) and (16), respectively.

$$\sum_{t\in\Psi^k}\{u_t^k\} = \delta^k;\ \forall k \in \{\mathcal{K}^{\mathrm{NI}} \cup \mathcal{K}^{\mathrm{I}}\} \tag{15}$$

$$\sum_{t\notin\Psi^k}\{u_t^k\} = 0;\ \forall k \in \{\mathcal{K}^{\mathrm{NI}} \cup \mathcal{K}^{\mathrm{I}}\} \tag{16}$$

The non-interruptible appliances need to incorporate equations (17) and (18) as well. The former impose continuity in their operation while the latter force to schedule these appliances just once within their specified time windows.

$$on_t^k - off_t^k = u_t^k - u_{t-1}^k;\ \forall t \in \mathcal{T}\backslash t > 1 \wedge k \in \mathcal{K}^{\mathrm{NI}} \tag{17}$$

$$\sum_{t\in\Psi^k}\{on_t^k\} = 1;\ \forall k \in \mathcal{K}^{\mathrm{NI}} \tag{18}$$

3.6 - Thermostatically-controlled appliances modelling

In this work, two kind of thermostatically-controlled appliances namely a heating-ventilation-air conditioner (HVAC) system and an electric water heater (EWH) are considered. In both cases, the respective temperatures are modelled using linearized differential equations, as explained in [39]. Hence, equation (19) models the instantaneous indoor temperature while the model (20), (21) represents the instantaneous hot water temperature.

$$\theta_{r|t}^{Air,in} = \left(1 - \frac{\Delta\tau}{10^3 \cdot m^{Air,in} \cdot Q^{Air,in} \cdot R}\right) \cdot \theta_{r|t-1}^{Air,in} + \frac{1}{10^3 \cdot m^{Air,in} \cdot Q^{Air,in} \cdot R} \cdot \hat{\theta}_{r|t-1}^{Air,out} + \frac{\left(p_{r|t-1}^{HVAC,h} - p_{r|t-1}^{HVAC,c}\right)}{0.000277 \cdot m^{Air,in} \cdot Q^{Air,in}} \cdot C^{HVAC};\ \forall r \in \mathcal{R} \wedge t \in \mathcal{T}\backslash t > 1 \tag{19}$$

$$\theta_{r|t+1}^{w,h} = \theta_{r|t}^{w,h} + p_{r|t}^{EWH} \cdot \eta^{EWH} \cdot C^{w,h} - \left(\theta_{r|t}^{Air,in} - \theta_{r|t}^{w,h}\right) e^{\left(\frac{-\Delta\tau}{R^{w,h} \cdot C^{w,h}}\right)};\ \forall r \in \mathcal{R} \wedge t \in \mathcal{T}\backslash t < \mathcal{T} \wedge \hat{v}_{r|t}^{w,h} = 0 \tag{20}$$

$$\theta_{r|t+1}^{w,h} = \frac{\theta_{r|t}^{w,h} \cdot \left(\overline{v}^{EWH} - \hat{v}_{r|t}^{w,h}\right) + \theta_{r|t}^{w,c} \cdot \hat{v}_{r|t}^{w,h}}{\overline{v}^{EWH}};\ \forall r \in \mathcal{R} \wedge t \in \mathcal{T}\backslash t < \mathcal{T} \wedge \hat{v}_{r|t}^{w,h} > 0 \tag{21}$$

The constraints (22) and (23) need to be imposed to upper bound the consumption of the HVAC unit and EWH to rated values, respectively; while (24) imposes complementarity in the heating and cooling modes of the HVAC system.

$$0 \leq p_{r|t}^{HVAC,i} \leq u_t^{HVAC,i} \cdot \overline{p}^{HVAC};\ \forall r \in \mathcal{R} \wedge t \in \mathcal{T} \wedge i \in \{h, c\} \tag{22}$$

$$p_{r|t}^{EWH} \leq \overline{p}^{\mathrm{EWH}};\ \forall r \in \mathcal{R} \wedge t \in \mathcal{T} \tag{23}$$

$$u_t^{HVAC,h} + u_t^{HVAC,c} \leq 1;\ \forall t \in \mathcal{T} \tag{24}$$

To keep the thermal comfort according users' requirements, the constraints (25) and (26) impose limits on the indoor and hot water temperatures, respectively. In the former expression, dead-bands are introduced to avoid the frequent operation of the HVAC system [35].

$$\theta^{HVAC,sp} - \theta^{HVAC,db} \leq \theta_{r|t}^{Air,in} \leq \theta^{HVAC,sp} + \theta^{HVAC,db}; \forall r \in \mathcal{R} \wedge t \in \mathcal{T} \tag{25}$$

$$\underline{\theta}^{EWH} \leq \theta_{r|t}^{w,h} \leq \overline{\theta}^{EWH};\ \forall r \in \mathcal{R} \wedge t \in \mathcal{T} \tag{26}$$

The HVAC and EWH models are completed imposing the initial and final temperatures by (27) and (28), since the models (19)-(21) are not defined at $t = 1$.

$$\theta_{r|\mathcal{T}(1)}^{Air,in} = \theta_{r|\mathcal{T}(\mathrm{end})}^{Air,in} = \theta^{HVAC,sp}; \forall r \in \mathcal{R} \tag{27}$$

$$\theta_{r|\mathcal{T}(1)}^{w,h} = \theta_{r|\mathcal{T}(\mathrm{end})}^{w,h} = \theta^{EWH,sp};\ \forall r \in \mathcal{R} \tag{28}$$

3.7 - Home balance

Finally, it is necessary to maintain the generation-demand balance at any time instant, which is ensured by imposing the constraint (29). It is noteworthy that the non-controllable appliances demand is considered an uncertain parameter in this model.

$$p_{r|t}^{Grid,b} + p_{r|t}^{BES,dch} + p_{r|t}^{PV} = \hat{p}_{r|t}^{NC} + p_{r|t}^{PEV} + p_{r|t}^{Grid,s} + p_{r|t}^{BES,ch} + p_{r|t}^{EWH} +$$

$$\sum_{i \in \{h,c\}} \left\{ p_{r|t}^{HVAC,i} \right\} + \sum_{k \in \{\mathcal{K}^{\mathrm{NI}} \cup \mathcal{K}^{\mathrm{I}}\}} \left\{ u_t^k \cdot \overline{p}^k \right\};\ \forall r \in \mathcal{R} \wedge t \in \mathcal{T} \tag{29}$$

4 - The developed solution procedure

One of the major contributions of this paper is to develop a HEM system immune against outages. To this end, a three-stage methodology is proposed, which is summarized in the flowchart of Fig. 3. In the new methodology, grid outages are considered unknown and are modelled using IGDT. This technique has been widely used in robust-oriented optimization problems [40] as well as in HEM-related tools [41]. However, this technique is considered in this work for modelling the grid outages in a novel way. Fig. 4 sketches the basic foundation of IGDT. As seen in this figure, IGDT assumes an upper bound for the concerned uncertainty, which could be obtained from forecast information or historical databases. Then, the intrinsic error that should be associated to the predicted value is modelled using the so-called uncertain radius, which stands for the deviation assumed in order to get a more robust solution. Intuitively, this approach can be straightforward employed for outages modelling, which can be conceived as an uncertainty and whose maximum feasible value can be easily calculated, as shown in subsequent sections. The developed multi-stage methodology aims at calculating the required information for proper IGDT modelling. Thus, the first step calculates the minimum energy cost whereas the second stage aims at calculating the maximum duration of outages for which the scheduling is still feasible. With this information, the final stage of the developed algorithm yields a home scheduling plan immune against outages. The minimum cost calculating at stage 1 serves to consider economy factors at stage 3. This way, immunity against outages is achieved without inadmissibly incrementing the cost, in contrast to other conventional tools.

The developed procedure does not ignore other uncertainties that are related with HEM problems, such as RTP, PV generation of non-controllable demand. However, to simplify the model, these uncertainties are modelled via scenarios, as customary [42]. This approach is justified in the fact that these uncertainties can be easily predicted using conventional techniques [32, 33]. Then, the associated forecast errors can be modelled using simple distribution functions and therefore the model can be simplified [30]. As result, the model developed in this paper can be considered an original hybridization of both stochastic programming and IGDT. The following sections detail each stage of the developed procedure.

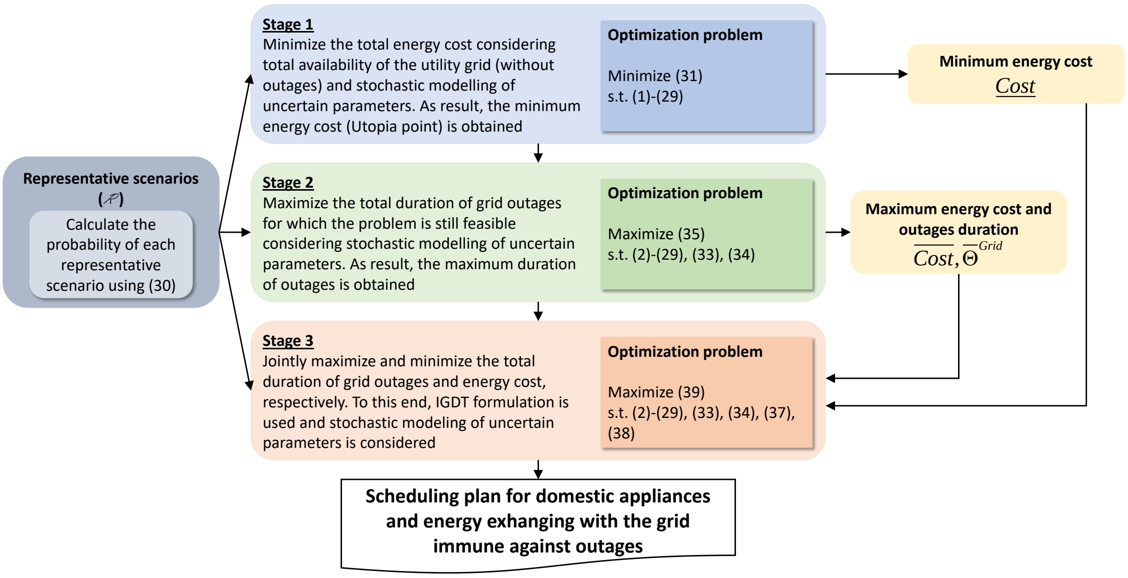

Fig. 3 - Flowchart of the developed solution procedure

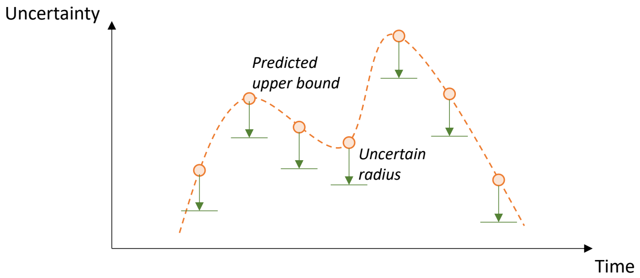

Fig. 4 - Sketch of IGDT modelling of uncertainties

4.1 - Stochastic modelling of uncertainties

In this paper, it is assumed that uncertain parameters can be predicted with sufficient accuracy. This is a reasonable assumption for the concerned uncertainties namely RTP, weather conditions and non-controllable appliances demand, since effective forecast techniques are widely studied and are available [43]. Assuming that uncertainties can be easily predicted, it is however suitable to model the possible forecast errors. These errors are caused by inevitably inaccuracies of forecast tools and can be modelled using Gaussian distributions, as pointed out in [44]. In this regard, it is noteworthy that uncertain parameters are not actually modelled using probability distributions. Instead, the forecast errors are modelled and a large number of scenarios are generated to catch the possible deviations from expected profiles. This approach has been already used in [44, 45], proving its suitability. Hence, Gaussian distribution is not used to model uncertainties such as solar irradiance, which is not reasonable [46], but more proper to represent forecast errors.

Using this approach, a large number of scenarios can be generated to catch the stochastic behavior of forecast errors. However, a large number of scenarios should be generated (~1,000 [47]), which may provoke intractability issues. To overcome this problem, cluster techniques have been widely used [42, 44]. Among the different tools available, the k-medoids technique is one of the most popular because its good features [48]. Basically, the k-medoids method groups the different scenarios into clusters, being possible to represent each cluster by only one of its members called medoid; this way, the number of scenarios can be drastically reduced without compromising the accuracy. In this paper, the methodology proposed in [49] has been followed to generate the representative scenarios using the k-medoid method, for which some helpful indexes (e.g. the Davies-Bouldin index) are used to determine the ideal number of clusters. For the sake of simplicity, Fig. 5 summarizes the process considered in this paper for stochastic modelling of uncertainties. Once the representative scenarios have been generated, the probability of each one is calculated as follows.

$$\pi_r = \frac{\mathrm{size}(\Omega_r)}{\mathrm{size}(\mathcal{S})};\ \forall r \in \mathcal{R} \tag{30}$$

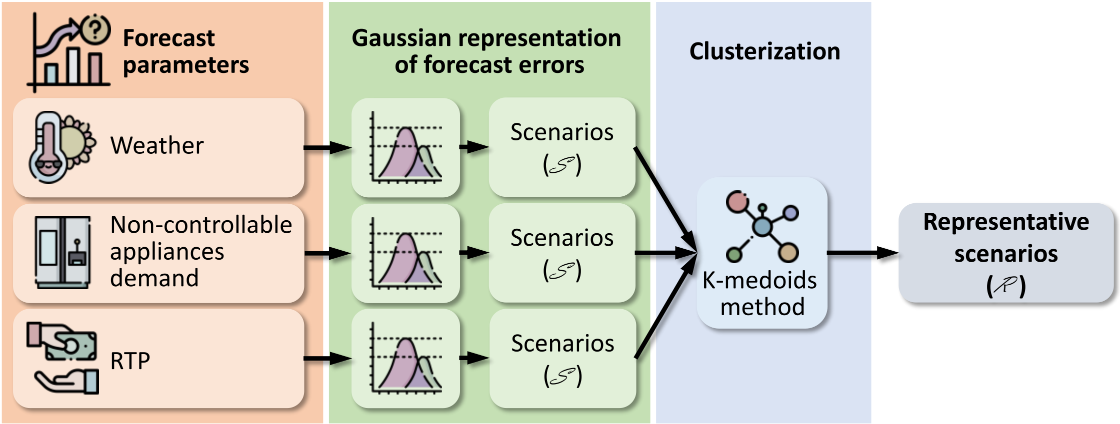

Fig. 5 - Flowchart of the process followed for stochastic representation of uncertainties

4.2 - Stage 1

The first stage of the developed methodology corresponds with the conventional stochastic-based HEM problem, which aims at minimizing the total energy cost considering stochastic modelling of uncertainties [30]. Also, it is necessary to include the operational and maintenance cost of the BES, since the battery lifetime strongly depends on the number of charging-discharging cycles [50]. With these premises, the total cost can be stated as follows

$$Cost = \sum_{r\in\mathcal{R}} \left\{\pi_r \cdot \sum_{t\in\mathcal{T}} \left\{\Delta\tau \cdot \left[\left(\hat{\lambda}_{r|t}^{Grid,b} \cdot p_{r|t}^{Grid,b} - \hat{\lambda}_{r|t}^{Grid,s} \cdot p_{r|t}^{Grid,s}\right) + \mu \cdot \left({p_{r|t}^{BES,ch}}^2 + {p_{r|t}^{BES,dch}}^2\right)\right]\right\}\right\} \quad (31)$$

It is worth noting that the energy price is considered unknown as RTP tariff is assumed for the installation. Also, the BES maintenance cost is stated proportional to the quadratic energy exchanged with the home, as pointed out in [51]. This model introduces nonlinearities because the quadratic charging and discharging BES powers. To keep the model linear, piecewise representations of the quadratic terms are used [52]. Hence, the first stage can be straightforward formulated as

$$\underline{Cost} \to \min_{x} Cost \quad (32)$$

Subject to: (1)-(29)

As result of the first stage, the minimum cost is obtained, which can be assimilated as the Utopia point in multi-objective problems [30]. This information is necessary for the IGDT process performed in posterior stages, for which the minimum cost marks the limit from which the expenditures can be incremented to make the scheduling plan more aware against grid outages.

4.3 - Stage 2

Now, the problem is focused on determining the maximum duration of grid outages for which the HEM scheduling is still feasible. It means, this stage aims to ask the following question: how long could be the home disconnected from the utility grid at most? To get a response, the HEM problem posed at Stage 1 should be reformulated to model the grid outages. To this end, the binary variable y_t^{Grid} is introduced, which is equal to 1 if the utility grid is available (no outage event) at time t and 0 otherwise. Thereby, the constraint (1) can be rewritten as

$$p_{r|t}^{Grid,i} \leq \underbrace{u_t^{Grid,i} \cdot y_t^{Grid}}_{\omega_t^{Grid,i}} \cdot \overline{p}^{Grid};\ \forall r \in \mathcal{R} \wedge t \in \mathcal{T} \wedge i \in \{b, s\} \tag{33}$$

In (33), the nonlinear product of two integer variables appear, which can be linearized introducing the pair of dummy variables $\omega_t^{Grid,i};\ i \in \{b, s\}$, and the following set of constraints [40].

$$\begin{cases} \omega_t^{Grid,i} \leq u_t^{Grid,i} \\ \omega_t^{Grid,i} \leq y_t^{Grid} \\ \omega_t^{Grid,i} \geq u_t^{Grid,i} + y_t^{Grid} - 1 \\ \omega_t^{Grid,i} \geq 0 \end{cases};\ \forall t \in \mathcal{T} \wedge i \in \{b, s\} \tag{34}$$

The reader can check that the model above allows to linearize the constraint (33). Thus, the total duration of grid outages can be calculated as follows

$$\Theta^{Grid} = \Delta\tau \cdot \left[\text{size}(\mathcal{T}) - \textstyle\sum_{t\in\mathcal{T}}\left\{\boldsymbol{y}^{Grid}\right\}\right], \boldsymbol{y}^{Grid} = \left[y_{\mathcal{T}(1)}^{Grid}, y_{\mathcal{T}(2)}^{Grid}, \dots, y_{\mathcal{T}(\text{end})}^{Grid}\right] \tag{35}$$

As mentioned, the objective of this stage is to calculate the maximum possible duration of grid outages, for which the following optimization problem is stated

$$\overline{\Theta}^{Grid}, \overline{Cost} \rightarrow \max_{x, y^{Grid}} \Theta^{Grid} \tag{36}$$

Subject to: (2)-(29), (33), (34)

It is worth noting that the maximum energy cost is obtained from (36) as by-product. This is logic since stage draws the most unfavourable situation, in which the grid is unavailable for the maximum time possible. Under this situation, more energy must be acquired from the grid to compensate the use of PV panels and BES to self-supply the home during outages, which inevitably increment the cost. This stage has therefore the objective of determining the upper bound of the uncertainties concerned (i.e. the duration of grid outages) but also the electricity bill. As seen in Fig. 4, this information is necessary for IGDT modelling, which is the approach used in this paper to model the possible grid blackouts.

4.4 - Stage 3

Although the previous stage yields a very robust scheduling against outages, it is expected to achieve such robustness at expenses of incrementing the energy cost. In practise, this result would be implausible since the total cost is an important concern. So that, home inhabitants may be unwilling to accept the scheduling result if it supposes incrementing the electricity bill beyond a limit. To solve this issue, the stage 3 aims at finding a compromise solution between robustness and economy. To that end, a novel IGDT-based formulation of the HEM problem has been developed. Basically, IGDT is a robust-oriented approach for optimization problem that finds the maximum deviation of uncertainties with respect to their predicted values [53]. This way, the result of the problem is immune against the effect of uncertainties. This principle is used in this work but in a novel way. Firstly, the total cost is modelled as an ‘artificial’ uncertainty, together the duration of grid outages, whereas the other uncertainties are modelled using simple stochastic programming, as commented before. This approach aims at jointly optimizing both the electricity bill and duration of grid outages, with the aim of obtaining a robust scheduling plan without incrementing the electricity bill beyond an assumable limit. This limit can be modelled as an uncertain radius associated with the energy cost. In addition, the upper and lower bounds of the electricity bill can be obtained in previous stages, so that modelling the total expenditures as an uncertainty does not suppose any extra computation. The following constraints model the variation of both the electricity cost and total duration of outage and relate them with their associated uncertain radiuses.

$$Cost(\boldsymbol{x}) \leq \overline{Cost} - \alpha^{Cost} \cdot \left(\overline{Cost} - \underline{Cost}\right) \tag{37}$$

$$\Theta^{Grid}\left(\boldsymbol{y}^{Grid}\right) \geq \alpha^{Grid} \cdot \overline{\Theta}^{Grid} \tag{38}$$

where α's $\in [0,1]$ are the so-called 'uncertain radiuses'. These variables measure the deviation of the cost and grid outages with respect to benchmark points. For example, in the case of the cost, it is clear that its value would lie between the maximum and minimum bounds calculated previously. Thereby, the value of α^{Cost} will determine the deviation of the cost with respect to its maximum value, which has been established as the benchmark point, but taking into account its limits. Consequently, it is easy to check that the higher α^{Cost} the lower cost. Actually, if $\alpha^{Cost} = 1$ the total cost will be equal to the minimum value calculated at stage 1, while the maximum value calculated at stage 2 would be observed if $\alpha^{Cost} = 0$. The reader can check that the similar principle has been established to model the duration of grid outages.

The inclusion of the radiuses α's as variables allows to easily establish the following optimization problem

$$\max_{\boldsymbol{x},\boldsymbol{y}^{Grid},\alpha^{Grid},\alpha^{Cost}} \alpha^{Grid} + \alpha^{Cost} \tag{39}$$

Subject to: (2)-(29), (33), (34), (37), (38) The optimization problem above aims at jointly maximizing both radiuses (i.e. α^{Grid} and α^{Cost}), which is equivalent to jointly maximize and minimize the grid outages and electricity bill, respectively. Indeed, if the value of α^{Grid} is maximized, the duration of grid outages is maximized as well by (38), while if the value of α^{Cost} is maximized, the total cost is minimized according to (37). Thereby, the robustness against outages is considered but without significantly incrementing the electricity bill. It is noteworthy that a lower bound can be imposed to α^{Cost} in order to establish a limit on the monetary expenditures that the users are willing to assume. However, this kind of limitation has not been considered in this paper in order to better illustrate the performance of the developed methodology.

5 - Case study

This section presents a case study and comments various numerical results in order to illustrate the performance of the developed methodology. In this regard, the developed computational model has been applied to a benchmark prosumer environment as described in Section 2. The problem has been solved over a 24 h time horizon with 30 min time resolution ($\Delta\tau = 0.5$). The mathematical models developed in previous sections have been coded under Matlab R2019a environment. The MILP optimization problem has been solved using Gurobi [54] on an Intel® Core™ i7-10700K (32 GB RAM). The experiments carried out by the authors revealed competitive computational efforts (10-15 minutes on average), which is assumable for HEM problems. On the other hand, the MILP structure of the mathematical formulation ensures its good scalability to larger problems and layouts, as the computational cost grows polynomially with the number of variables and constraints [55].

5.1 - Input data

For the uncertain parameters (i.e. RTP, weather parameters and non-controllable appliances demand), real data have been considered. The purchasing and selling energy prices were observed at the PJM FE Ohio on July 1 and 9, 2019, respectively [54]. The weather parameters (solar irradiance and temperature) correspond with real data measured at Virgin Islands on May 3, 2016 [57]. Lastly, the non-controllable appliances and hot water demand have been taken from [49]. Fig. 6 plots the considered uncertain profiles besides the generated 15 representative scenarios based on assumable forecast errors. To construct the representative space, up to 1,000 scenarios were generated assuming Gaussian distribution of errors and standard deviations of 0.3, 0.05, 0.4, 0.35 and 0.2 for solar irradiance, temperature, RTP, non-controllable appliances demand and hot water consumption, respectively. The value of standard deviations has been set according to heuristic criteria, in order to properly represent the forecast errors of the different uncertainties. Indeed, as one can see in Fig. 6, the generated scenarios cover a wide range of possible deviations from expected profiles and, therefore, stochastic character of uncertainties has been properly assumed.

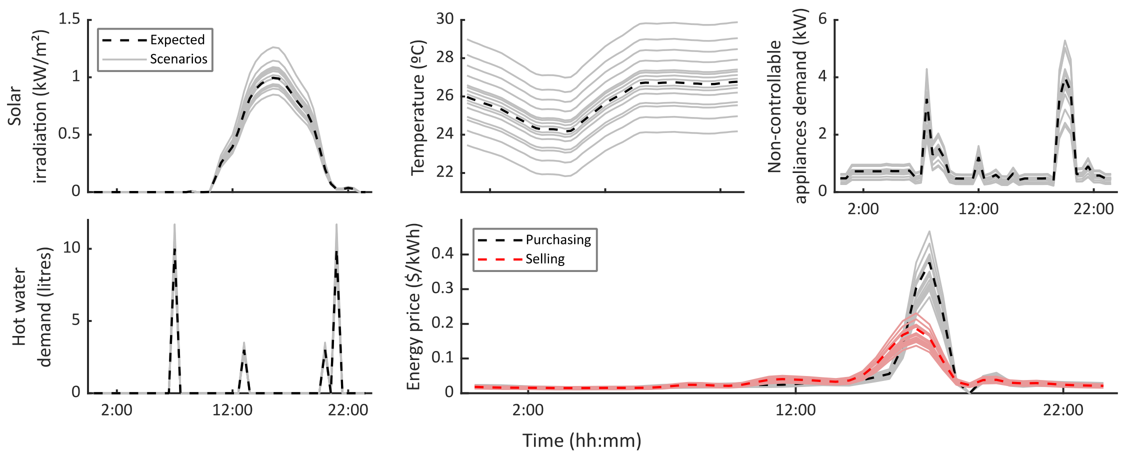

Fig. 6 - Expected profiles and generated representative scenarios for the uncertain parameters

A small-scale PV array and a Li-ion battery pack are deployed. The peak power of the PV array and BES capacity have been considered variable for simulation purposes, while the remainder data of these assets have been extracted from [49, 51, 58] and are collected in Table 2. The data of the thermostatically-controlled appliances can be found in [34, 59] and are reported in Tables 3 and 4 for the HVAC system and EWH system, respectively. On the other hand, the thermal data of the building can be found in [34].

Table 2 - Data of PV array and BES [49, 51, 58]

Parameter	Value
$\overline{p}^{BES}$	50% of the nominal capacity
η^{PV}	0.167 pu
μ	10^{-6} kWh²
$\underline{\varepsilon}^{BES}$	60% of the nominal capacity

Table 3 - Data of the HVAC system [26, 34]

Parameter	Value
$\overline{p}^{HVAC}$	2 kW
C^{HVAC}	1.2
$\theta^{HVAC,sp/db}$	23/0.5 ºC

Table 4 - Data of the EWH [34, 59]

Parameter	Value
$\overline{p}^{EWH}$	2.1 kW
η^{EWH}	0.9 pu
$\overline{v}^{EWH}$	50 gal
$R^{w,h}$	863.4 ºC/kWh
$C^{w,h}$	1.52 ºC/kW
$\underline{\theta}^{EWH}/\overline{\theta}^{EWH}/\theta^{w,c}$	45/60/10 ºC

Four different controllable appliances have been considered, whose relevant data have been adapted from [42] and are collected in Table 5. A 22-kWh Renault Zoe with a 3-kW charging/discharging power limitation has been considered. The efficiency of the on-board battery bank has been assumed equal to 98%, which is a reasonable value for Li-ion batteries [50]. Although the vehicle could be parked earlier, it is assumed that an intelligent control system manages its charging process. This kind of tools enables the charging process at 0:00 h [38], to take advantage of low energy prices and avoid high peak demands due to aggregated charging profiles. Following this idea, the electric vehicle could not be charged beyond 9:30 h. Lastly, it is assumed that the initial SOC of the on-board storage system is 40% of its nominal capacity.

Table 5 - Characteristics of the controllable appliances [36]

Appliance	Power (kW)	δ (hrs.)	Ψ	Type
Dishwasher	2.5	2	1:00-18:00	Interruptible
Washing machine	3	3	1:00-12:00	Non-interruptible
Spin dryer	2.5	1	13:00-21:00	Interruptible
Vacuum cleaner	1.2	0.5	8:30-16:00	Non-interruptible

5.2 - Results

In order to show how the developed methodology works, Fig. 7 plots the total cost at different stages with various PV and BES sizes. From this figure, it can be observed that the economy of the system is improved as the rated values of the PV array and battery bank grows. As expected, stage 1 yielded the minimum cost in any case. This stage finds the minimum electricity bill, since this information is necessary for posterior stages. In contrast, the maximum expenditures were observed at stage 2. This step aims at calculating the maximum duration of outages for which the system is still feasible. In this regard, the stage 2 supposes the most unfavourable situation in which the grid is largely unavailable. Nevertheless, this pessimistic situation can be contemplated at expense of incrementing the electricity bill. This situation may be not assumable by users, that might be unwilling to pay more for considering reliability. Actually, up to 10 outage hours can be assumed, but incrementing the bill by ~30 %. In this regard, stage 3 jointly optimizes both the energy cost and grid outages, with the aim of obtaining a robust scheduling plan without notably incrementing the bill. This is clearly observed in Fig. 7, where it is observed how the total cost calculated at stage 3 always lied between the results obtained at stage 2 and 1. This is better appreciated in Fig. 8, where the total outages duration is depicted for different PV and BES sizes. As observed, the outages duration is usually longer at stage 2, since this stage is devoted on calculating the maximum outages duration for which the problem is feasible yet. On the other hand, stage 3 frequently contemplated shorter outages, thus proving that this stage achieves a compromise among economy and robustness. In fact, stage 3 is able to assume up to 6.5 outage hours without incrementing the electricity bill, as observed in Fig. 7. This result evidences the capability of the developed procedure to obtain a result immune against outages, whereas economic concerns are also considered on a whole. Finally, it is noteworthy that the higher PV and BES sizes the longer outage is admissible, which is expected since self-supplying of the installation is directly related with the capacity of the onsite assets.

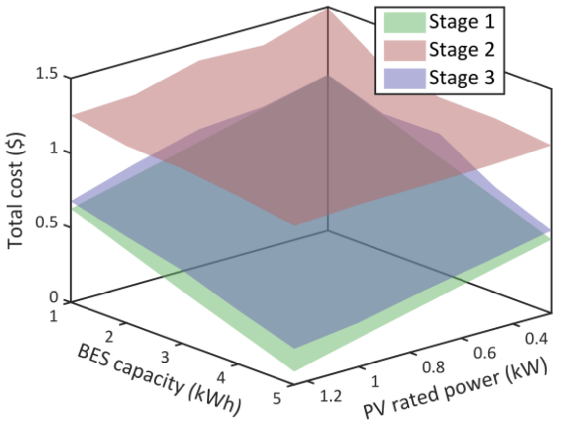

Fig. 7 - Total cost at different stages of the developed methodology with different PV and BES sizes

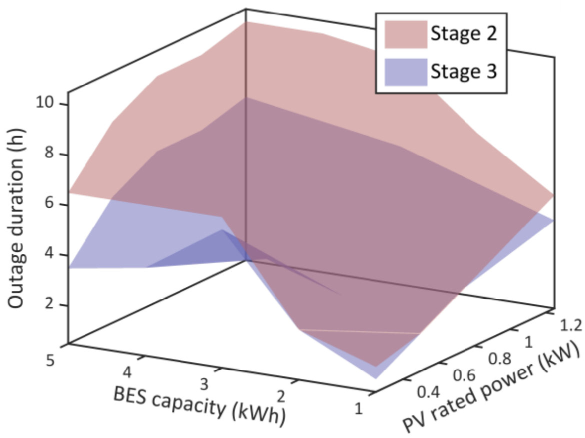

Fig. 8 - Total outage duration at different stages of the developed methodology with different PV and BES sizes

Improving the economy of the system is directly related with the exchanging energy with the utility grid. In this regard, Fig. 9 plots the total energy purchased from the grid at different stages for different sizes of PV and BES. At stage 1, the acquired energy grows with the battery capacity. This is due to the scheduler tends to buy more energy from the grid as more storage is available to get a better monetary performance from batteries, i.e. buy energy at low-price periods to consume it during peak periods or even sell it to the utility grid. In contrast, the total purchased energy decreases as the PV rated power grows. This is logic since the home becomes more self-sufficient as the PV array grows, thus requiring less energy from the grid. The same behaviour can be appreciated at stage 3, however, the total purchased energy is less sensitive to the size of onsite assets in this case. This is due to both stages aims at minimizing the total cost, however, this objective is not lonely optimized at stage 3, when the grid outages are also minimized. In fact, at stage 2, when the total outages duration is only maximized, the energy purchased from the grid is practically unsensitive with the BES capacity, since in this case the total cost is irrelevant. Similar behaviour is observed with the energy sold in Fig. 10. In this case, the results for stage 2 are not plotted because the total energy sold to the grid was zero. This result is logic since this stage is performed regardless the electricity bill, being unnecessary selling energy to the grid. Regarding the stages 1 and 3, it can be observed that the total energy that is sold to the gird grows with the PV and BES capacities, which is a coherent result as explained above.

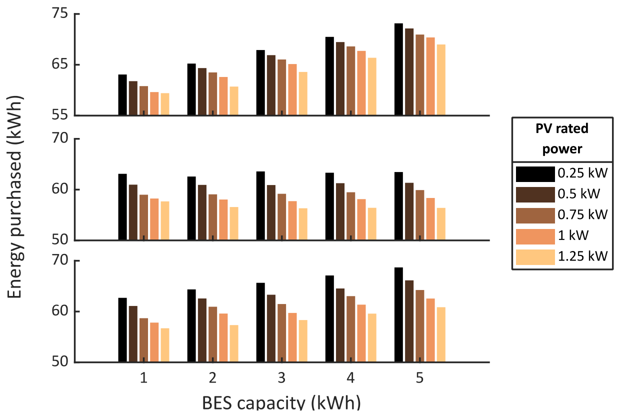

Fig. 9 - Total energy purchased from the utility grid at stage 1 (upper), 2 (middle) and 3 (bottom) of the developed methodology, with different PV and BES sizes

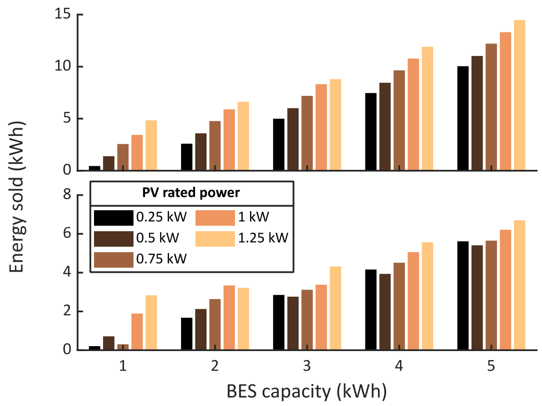

Fig. 10 - Total energy sold to the utility grid at stage 1 (upper) and 3 (bottom) of the developed methodology, with different PV and BES sizes

To get a better view into the performance of the developed scheduler, Fig. 11 shows the scheduling result for the energy exchanging with the grid. In this figure, the duration of the grid outages is also plotted for a further analysis. As observed, during a grid outage (at stages 2 and 3), the home does not exchange energy with the grid, which demonstrates that the developed tool is able to effectively model a shutdown of the utility grid. This figure also allows to analyse how the scheduling result is performed depending on the stage. Hence, at stage 1, a considerable amount of energy is sold in order to improve the economy of the system, which is the unique objective at this stage. Central hours of the day are especially exploited for that, taking advantage of high PV potential. This capability is notably limited at stage 3, since in this case an outage event precludes selling energy when the PV potential is high. This is due to the total cost is not the unique objective at this stage, and the outages duration are also maximized to get a robust scheduling result. Finally, the home does not sell energy to the grid at stage 3, since the unique objective is the maximization of the grid outages in this case.

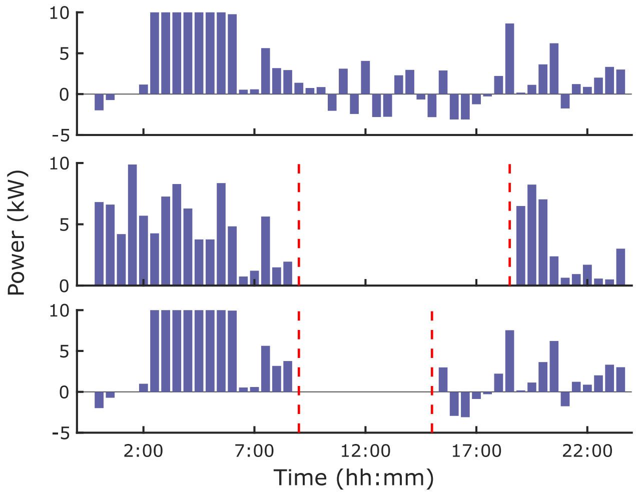

Fig. 11 - Scheduling result for the utility grid at stage 1 (upper), 2 (middle) and 3 (bottom) of the developed methodology, taking $\overline{p}^{PV} = 1\ kW$ and $\overline{\varepsilon}^{BES} = 5\ kWh$. In this figure, negative values mean sold power while the outages are delimited by red discontinuous lines

The storage capacity plays a vital role during an outage event, since it is responsible (besides the onsite generation) to supply the home demand when the utility grid is not available. In this regard, Fig. 12 plots the scheduling result for the different storage banks (BES and PEV) at different stages. As observed, at stage 1 the BES is mainly focused on reducing the total cost. To this end, the battery pack is partially discharged during noon as well as at evening, when large PV potential is also exploited to sell energy to the grid, as seen in Fig. 11. When a large outage is expected at stage 2, PEV is rapidly charged and energy stored in BES is preserved for supplying the home during outage. This is obviously a very robust and pessimistic perspective which notably deteriorates the economy of the home. This scheduling profile is adjusted at stage 3, when the outage events are shorter and BES can be further exploited to further reduce the total cost of the system.

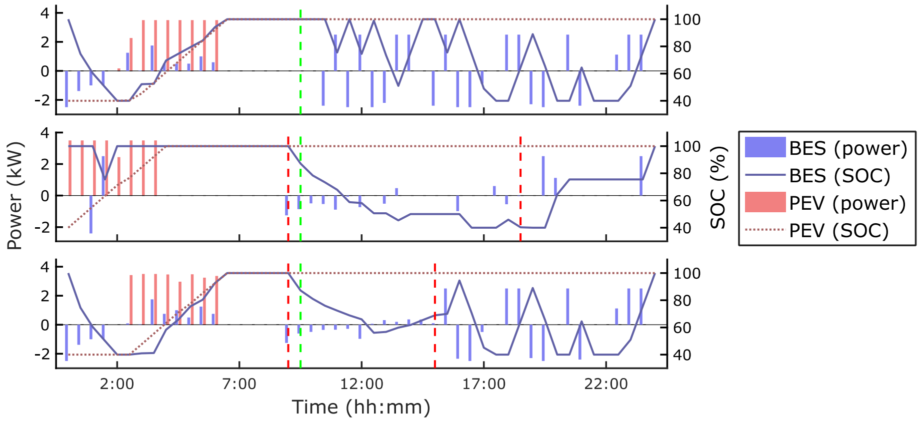

Fig. 12 - Scheduling result for the storage systems at stage 1 (upper), 2 (middle) and 3 (bottom) of the developed methodology, taking $\overline{p}^{PV} = 1\ kW$ and $\overline{\varepsilon}^{BES} = 5\ kWh$. In this figure, negative values mean discharging powers. The outages and PEV time window are delimited by red and green discontinuous lines, respectively

Lastly, Fig. 13 shows the scheduling result for the controllable appliances at different stages. As seen in this figure, the controllable appliances are normally scheduled during dawn, when the energy price is quite low. For the appliances that cannot be scheduled during early morning (vacuum cleaner and dryer), the algorithm responds different if an outage is expected or not. If the algorithm prevents an outage, it firstly calculates the most unfavourable, then the appliances are scheduling during those hours in which the grid is available. At stage 3, the vacuum cleaner is scheduled during morning, when the energy price is still low. This operational principle shows that those hours with high PV penetration (evening), are more economic to sell energy to the grid, taking advantage of high selling pricing. This is the reason why the controllable appliances are not scheduled during those hours.

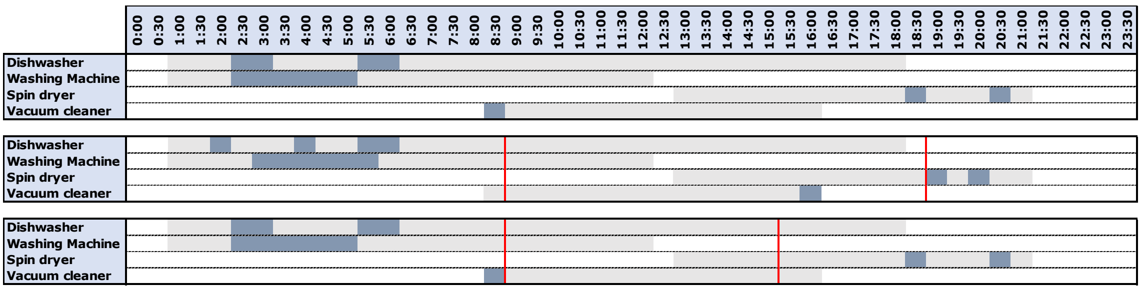

Fig. 13 - Scheduling result for the controllable appliances at stage 1 (upper), 2 (middle) and 3 (bottom) of the developed methodology, taking $\overline{p}^{PV} = 1\ kW$ and $\overline{\varepsilon}^{BES} = 5\ kWh$. In this figure, the outages are delimited by red discontinuous lines, while the time windows are denoted by grey shaded areas

6 - Conclusions

A novel HEM model has been presented in this paper. The novel proposal is robust against outages. To this end, a novel stochastic-IGDT formulation has been proposed and a three-stage solution methodology has been developed. The new model incorporates some uncertainties via scenarios while the grid outages are included using IGDT. The consideration of weather uncertainties allows to optimize the control of rooftop PV panels to improve both economy and reliability of the system. The three-stage developed procedure allows to optimize the total cost of the system while possible outage events are considered on a whole, this way, the result obtained can be considered immune against outages. Moreover, the whole presented formulation is MILP, being efficiently solvable using conventional solvers.

A case study has been presented on a benchmark prosumer environment to validate the proposed HEM tool. Results served to prove the effectiveness of the developed formulation to model grid outages. The performance of the solution procedure has been also illustrated, showing the results obtained at each stage and how the total cost of the system is further optimized jointly considering grid outages. The scheduling results at different stages has been also commented, highlighting the role of the different home assets during grid outages, especially storage systems, onsite generators and controllable appliances, whose scheduling can be adjusted in order to prevent possible shutdowns. Furthermore, the optimal control of PV panels in concordance with storage assets and controllable appliances allows to reduce the impact of outages without notably incrementing the electricity bill, at least beyond a reasonable threshold. This last result evidences the capability of the developed tool to maximize the welfare of home inhabitants since, together the minimization of the electricity bill, the impact of grid failures is also reduced, minimizing its possible harmful effects on people’s routines.

Ongoing works are focused on applying the developed formulation to planning tools, in order to optimally design the active home assets considering grid outages. The ideas exposed here will be also implemented in other similar management tools related with microgrids.

Acknowledgments

The icons used in the figures throughout this paper were developed by Freepik, from www.flaticon.com.

References

[1] European Association for external thermal insulation composite systems. European energy saving guide. 2016. Online, available at: http://www.ea-etics.eu, (accessed Jan. 18, 2021).

[2] European Union. Directive 2010/31/EU of the European parliament and of the council of 19 may 2010 on the energy performance of buildings (recast). 2010.

[3] International Energy Agency. World Energy Outlook 2020. Online, available at: https://www.iea.org/reports/world-energy-outlook-2020, (accessed Jan. 18, 2021).

[4] H. Shareef, M.S. Ahmed, A. Mohamed, E. Al Hassan. Review on home energy management system considering demand responses, smart technologies, and intelligent controllers. *IEEE Access* 2018; 6: 24498-509. https://doi.org/10.1109/ACCESS.2018.2831917.

[5] K. Wooton. E Source market research reveals that power outages cost businesses over $27 billion annually, winter storm Jonas makes it worse. E Source; Jan. 27, 2016. Online, available at: https://www.esource.com/ES-PR-Outages-2016-01/Press-Release/Outages, (accessed Jan. 18, 2021).

[6] X. Wang, X. Mao, H. Khodaei. A multi-objective home energy management system based on internet of things and optimization algorithms. *Journal of Building Engineering* 2021; 33: 101603. https://doi.org/10.1016/j.jobe.2020.101603.

[7] S.B. Slama. Design and implementation of home energy management system using vehicle to home (H2V) approach. *Journal of Cleaner Production* 2021; 312: 127792. https://doi.org/10.1016/j.jclepro.2021.127792.

[8] G. Van de Kaa, S. Stoccuto, C.V. Calderón. A battle over smart standards: Compatibility, governance, and innovation in home energy management systems and smart meters in the Netherlands. *Energy Research & Social Science* 2021; 82: 102302. https://doi.org/10.1016/j.erss.2021.102302.

[9] Z. Zhao, W. C. Lee, Y. Shin, K. Song. An Optimal Power Scheduling Method for Demand Response in Home Energy Management System. *IEEE Transactions on Smart Grid* 2013; 4(3): 1391-400. https://doi.org/10.1109/TSG.2013.2251018.

[10] D. Niyato, L. Xiao, P. Wang. Machine-to-machine communications for home energy management system in smart grid. *IEEE Communications Magazine* 2011; 49(4): 53-9. https://doi.org/10.1109/MCOM.2011.5741146.

[11] J. Ma, H.H. Chen, L. Song, Y. Li. Residential Load Scheduling in Smart Grid: A Cost Efficiency Perspective. *IEEE Transactions on Smart Grid* 2016; 7(2): 771-84. https://doi.org/10.1109/TSG.2015.2419818.

[12] I.-Y. Joo, D.-H. Choi. Optimal household appliance scheduling considering consumer's electricity bill target. *IEEE Transactions on Consumer Electronics* 2017; 63(1): 19-27. https://doi.org/10.1109/TCE.2017.014666.

[13] B. Lokeshgupta, S. Sivasubramani. Cooperative game theory approach for multi-objective home energy management with renewable energy integration. *IET Smart Grid* 2019; 2(1): 34-41. https://doi.org/10.1049/iet-stg.2018.0094.
[14] Y. Liu, Y. Zhang, K. Chen, S. Z. Chen, B. Tang. Equivalence of Multi-Time Scale Optimization for Home Energy Management Considering User Discomfort Preference. IEEE Transactions on Smart Grid 2017; 8(4): 1876-87. https://doi.org/10.1109/TSG.2015.2510222.
[15] B. Lokeshgupta, S. Sivasubramani. Multi-objective home energy management with battery energy storage systems. *Sustainable Cities & Society* 2019; 47: 101458. https://doi.org/10.1016/j.scs.2019.101458.
[16] Duman AC, Erden HS, Gönül Ö, Güler Ö. A home energy management system with an integrated smart thermostat for demand response in smart grids. Sustainable Cities and Society. 2021 Feb 1; 65:102639. https://doi.org/10.1016/j.scs.2020.102639.
[17] Javadi MS, Nezhad AE, Jordehi AR, Gough M, Santos SF, Catalão JP. Transactive energy framework in multi-carrier energy hubs: A fully decentralized model. Energy. 2022 Jan 1; 238:121717. https://doi.org/10.1016/j.energy.2021.121717
[18] Ghazvini MA, Lipari G, Pau M, Ponci F, Monti A, Soares J, Castro R, Vale Z. Congestion management in active distribution networks through demand response implementation. Sustainable Energy, Grids and Networks. 2019 Mar 1; 17:100185. https://doi.org/10.1016/j.segan.2018.100185.
[19] Manshadi SD, Khodayar ME. Resilient operation of multiple energy carrier microgrids. IEEE Transactions on Smart Grid. 2015, 24; 6(5): 2283-92. https://doi.org/10.1109/TSG.2015.2397318
[20] Masrur H, Gamil MM, Islam MR, Muttaqi KM, Lipu MH, Senjyu T. An Optimized and Outage-resilient Energy Management Framework for Multi-carrier Energy Microgrids Integrating Demand Response. IEEE Transactions on Industry Applications. 2022 Mar 18. https://doi.org/10.1109/TIA.2022.3160683.
[21] Tuttle DP, Fares RL, Baldick R, Webber ME. Plug-In Vehicle to Home (V2H) duration and power output capability. In 2013 IEEE Transportation Electrification Conference and Expo (ITEC) 2013 Jun 16 (pp. 1-7). IEEE. https://doi.org/10.1109/ITEC.2013.6574527
[22] Y. Yang, S. Wang. Resilient residential energy management with vehicle-to-home and photovoltaic uncertainty. *International Journal of Electrical Power & Energy Systems* 2021; 132: 107206. https://doi.org/10.1016/j.ijepes.2021.107206.
[23] F. Zhang, F. Luo, Z. Dong, Y. Liu, G. Ranzi. Hierarchical energy management scheme for residential communities under grid outage event. *IET Smart Grid* 2020; 3(2): 174-81. https://doi.org/10.1049/iet-stg.2019.0150.
[24] R. Roche, F. Berthold, F. Gao, F. Wang, A. Ravey, S. Williamson. A model and strategy to improve smart home energy resilience during outages using vehicle-to-home. *2014 IEEE International Electric Vehicle Conference (IEVC)* 2014: 1-6. https://doi.org/10.1109/IEVC.2014.7056106.
[25] M.W. Tian, P. Talebizadehsardari. Energy cost and efficiency analysis of building resilience against power outage by shared parking station for electric vehicles and demand response program. *Energy* 2021; 215: 119058. https://doi.org/10.1016/j.energy.2020.119058.
[26] S.A. Mansouri, A. Ahmarinejad, E. Nematbakhsh, M.S. Javadi, A.R. Jordehi, J.P.S. Catalão. Energy management in microgrids including smart homes: A multi-objective approach, *Sustainable Cities & Society* 2021; 69: 102852. https://doi.org/10.1016/j.scs.2021.102852.
[27] P. Lubello, F. Papi, A. Bianchini, C. Carcasci. Considerations on the impact of battery ageing estimation in the optimal sizing of solar home battery systems. *Journal of Cleaner Production* 2021; 329: 129753. https://doi.org/10.1016/j.jclepro.2021.129753.
[28] K. Aurangzeb, S. Aslam, H. Herodotou, M. Alhussein, S.I. Haider. Towards Electricity Cost Alleviation by Integrating RERs in a Smart Community: A Case

Study. *2019 23rd International Conference Electronics*; Palanga, Lithuania 2019: 1-6. https://doi.org/10.1109/ELECTRONICS.2019.8765693.

[29] J.P. Wesche, E. Dütschke. Organisations as electricity agents: Identifying success factors to become a prosumer. *Journal of Cleaner Production* 2021; 315: 127888. https://doi.org/10.1016/j.jclepro.2021.127888.

[30] M. Tostado-Véliz, S. Gurung, F. Jurado. Efficient solution of many-objective Home Energy Management systems. *International Journal of Electrical Power & Energy Systems* 2022; 136: 107666. https://doi.org/10.1016/j.ijepes.2021.107666.

[31] M.S. Javadi, et al. Self-scheduling model for home energy management systems considering the end-users discomfort index within price-based demand response programs. *Sustainable Cities & Society* 2021; 68: 102792. https://doi.org/10.1016/j.scs.2021.102792.

[32] A. Naz, N. Javaid, M.B. Rasheed, A. Haseeb, M. Alhussein, K. Aurangzeb. Game Theoretical Energy Management with Storage Capacity Optimization and Photo-Voltaic Cell Generated Power Forecasting in Micro Grid. *Sustainability* 2019; 11: 2763. https://doi.org/10.3390/su11102763.

[33] K. Aurangzeb et al. Energy forecasting using multiheaded convolutional neural networks in efficient renewable energy resources equipped with energy storage system. *Transactions on Emerging Telecommunications Technologies* 2022; 33(2): e3837. https://doi.org/10.1002/ett.3837.

[34] N. G. Paterakis, O. Erdinç, A.G. Bakirtzis, J.P.S. Catalão. Optimal Household Appliances Scheduling Under Day-Ahead Pricing and Load-Shaping Demand Response Strategies. *IEEE Transactions on Industrial Informatics* 2015; 11(6): 1509-19. https://doi.org/10.1109/TII.2015.2438534.

[35] M. Tostado-Véliz, M. Bayat, A.A. Ghadimi, F. Jurado. Home energy management in off-grid dwellings: Exploiting flexibility of thermostatically controlled appliances. *Journal of Cleaner Production* 2021; 310: 127507. https://doi.org/10.1016/j.jclepro.2021.127507.

[36] S. Mandal, B.K. Das, N. Hoque. Optimum sizing of a stand-alone hybrid energy system for rural electrification in Bangladesh. *Journal of Cleaner Production* 2018; 200: 12-27. https://doi.org/10.1016/j.jclepro.2018.07.257.

[37] M. Tostado-Véliz, P. Arévalo, F. Jurado. An optimization framework for planning wayside and on-board hybrid storage systems for tramway applications. *Journal of Energy Storage* 2021; 43: 103207. https://doi.org/10.1016/j.est.2021.103207.

[38] H. -M. Chung, S. Maharjan, Y. Zhang, F. Eliassen. Intelligent Charging Management of Electric Vehicles Considering Dynamic User Behavior and Renewable Energy: A Stochastic Game Approach. *IEEE Transactions on Intelligent Transportation Systems* 2021; 22(12): 7760-71. https://doi.org/10.1109/TITS.2020.3008279.

[39] M. Javadi, et al. Optimal Operation of Home Energy Management Systems in the Presence of the Inverter-based Heating, Ventilation and Air Conditioning System. *2020 IEEE International Conference on Environment and Electrical Engineering and 2020 IEEE Industrial and Commercial Power Systems Europe (EEEIC / I&CPS Europe)* 2020; 1-6. https://doi.org/10.1109/EEEIC/ICPSEurope49358.2020.9160629.

[40] A.R. Jordehi. Information gap decision theory for operation of combined cooling, heat and power microgrids with battery charging stations. *Sustainable Cities & Society* 2021; 74: 103164. https://doi.org/10.1016/j.scs.2021.103164.

[41] A. Najafi-Ghalelou, S. Nojavan, K. Zare. Robust thermal and electrical management of smart home using information gap decision theory. *Applied Thermal Engineering* 2018; 132: 221-32. https://doi.org/10.1016/j.applthermaleng.2017.12.086.

[42] M.S. Javadi, et al. Optimal self-scheduling of home energy management system in the presence of photovoltaic power generation and batteries. *Energy* 2020; 210: 118568. https://doi.org/10.1016/j.energy.2020.118568.

[43] A. Masood, K. Ahmad. A review on emerging artificial intelligence (AI) techniques for air pollution forecasting: Fundamentals, application and performance. *Journal of*

Cleaner Production 2021; 322: 129072. https://doi.org/10.1016/j.jclepro.2021.129072.

[44] M. Mansour-Lakouraj, H. Niaz, J.J. Liu, P. Siano, A. Anvari-Moghaddam. Optimal risk-constrained stochastic scheduling of microgrids with hydrogen vehicles in real-time and day-ahead markets. *Journal of Cleaner Production* 2021; 318: 128452. https://doi.org/10.1016/j.jclepro.2021.128452.

[45] X. Xu et al. Optimal operational strategy for an offgrid hybrid hydrogen/electricity refueling station powered by solar photovoltaics. *Journal of Power Sources* 2020; 451: 227810. https://doi.org/10.1016/j.jpowsour.2020.227810.

[46] M. Aien, A. Hajebrahimi, M. Fotuhi-Firuzabad. A comprehensive review on uncertainty modeling techniques in power system studies. Renewable and Sustainable Energy Reviews 2016; 57: 1077-89. https://doi.org/10.1016/j.rser.2015.12.070.

[47] H. Rashidizadeh-Kermani, M. Vahedipour-Dahraie, A. Anvari-Moghaddam, J.M. Guerrero. A stochastic bi-level decision-making framework for a load-serving entity in day-ahead and balancing markets. *International Transactions on Electrical Energy Systems* 2019; 29(11): e12109. https://doi.org/10.1002/2050-7038.12109.

[48] E.S. Pinto, L.M. Serra, A. Lázaro. Evaluation of methods to select representative days for the optimization of polygeneration systems. *Renewable Energy* 2020; 151: 488-502. https://doi.org/10.1016/j.renene.2019.11.048.

[49] M. Tostado-Véliz, R.S. León-Japa, F. Jurado. Optimal electrification of off-grid smart homes considering flexible demand and vehicle-to-home capabilities. *Applied Energy* 2021; 298: 117184. https://doi.org/10.1016/j.apenergy.2021.117184.

[50] I. Alsaidan, A. Khodaei, W. Gao. A Comprehensive Battery Energy Storage Optimal Sizing Model for Microgrid Applications. *IEEE Transactions on Power Systems* 2018; 33(4): 3968-80. https://doi.org/10.1109/TPWRS.2017.2769639.

[51] F. Garcia-Torres, D.G. Vilaplana, C. Bordons, P. Roncero-Sánchez, M.A. Ridao. Optimal Management of Microgrids With External Agents Including Battery/Fuel Cell Electric Vehicles. *IEEE Transactions on Smart Grid* 2019; 10(4): 4299-308. https://doi.org/10.1109/TSG.2018.2856524.

[52] M. Tostado-Véliz, S. Kamel, H.M. Hasanien, R.A. Turky, F. Jurado. A mixed-integer-linear-logical programming interval-based model for optimal scheduling of isolated microgrids with green hydrogen-based storage considering demand response. *Journal of Energy Storage* 2022; 48: 104028. https://doi.org/10.1016/j.est.2022.104028.

[53] Y. Ben-Haim. Info-Gap Decision Theory - Decisions Under Severe Uncertainty, 2nd ed. Boston, MA: Academic Press, 2006. https://doi.org/10.1016/B978-0-12-373552-2.X5000-0.

[54] Gurobi Optimization L.L.C. Gurobi Optimizer Reference Manual, 2021. Online, available at: https://www.gurobi.com, (accessed Jan. 14, 2022).

[55] I.A. Avramidis, F. Capitanescu, G. Deconinck. A generic multi-period optimal power flow framework for combating operational constraints via residential flexibility resources. *IET Generation, Transmission & Distribution* 2021; 15(2): 306-20. https://doi.org/10.1049/gtd2.12022.

[56] Engie. Historical data reports. Online, available at: https://www.engieresources.com/historical-data#reports_anchor, (accessed Jan. 14, 2022).

[57] NOAA. Land base datasets. Online, available at: https://www.ncdc.noaa.gov/data-access/land-based-station-data/land-based-datasets, (accessed Jan. 14, 2022).

[58] M. Tostado-Véliz, P. Arévalo, F. Jurado. A comprehensive electrical-gas-hydrogen Microgrid model for energy management applications. *Energy Conversion & Management* 2021; 228: 113726. https://doi.org/10.1016/j.enconman.2020.113726.

[59] P. Du, N. Lu. Appliance Commitment for Household Load Scheduling. *IEEE Transactions on Smart Grid* 2011; 2(2): 411-9. https://doi.org/10.1109/TSG.2011.2140344.